

## Microengineering of a Three-Dimensional Heart on Chip Tissue Model

J Veldhuizen<sup>1</sup>, J Cutts<sup>1</sup>, Z Camacho<sup>1</sup>, D Brafman<sup>1</sup>, R Migrino<sup>2</sup>, and M Nikkhah<sup>1\*</sup>

<sup>1</sup>School of Biological and Health Systems Engineering, Arizona State University, Tempe, AZ

<sup>2</sup>Phoenix Veteran Affairs Health Care System, Phoenix, AZ

**Introduction:** Cardiovascular diseases persistently remain the main cause of mortality among people worldwide, despite substantial effort in research and therapeutic interventions. This limited success may be due to the lack of thorough understanding of mechanisms in disease progression. Currently, the gold standard for understanding these mechanisms is reliant mainly on animal models. However, animal models may lack physiological relevancy to humans, with the inability to precisely control microenvironmental cues for cellular and molecular level studies. In that regard, there is a crucial need for a biomimetic human heart tissue model, which can complement animal studies in recapitulating the pathophysiological characteristics of common cardiac diseases. In this work, we describe development of a physiologically relevant cardiac tissue model consisting of highly organized co-culture of cardiac cells within a precise microengineered platform. We aim to accurately model the architecture and cellular constituents of the native myocardium over long period of culture for cardiac biology and pharmacological studies.

**Materials and Methods:** The 3D microfluidic model is comprised of microposts to induce alignment of hydrogels-encapsulated tissues within the system. Neonatal rat cardiomyocytes (CMs) and cardiac fibroblasts (CFs) were encapsulated in Fibrin: Collagen I gel, loaded into the microfluidic device, and cultured for 14 days (Fig. 1A, B).

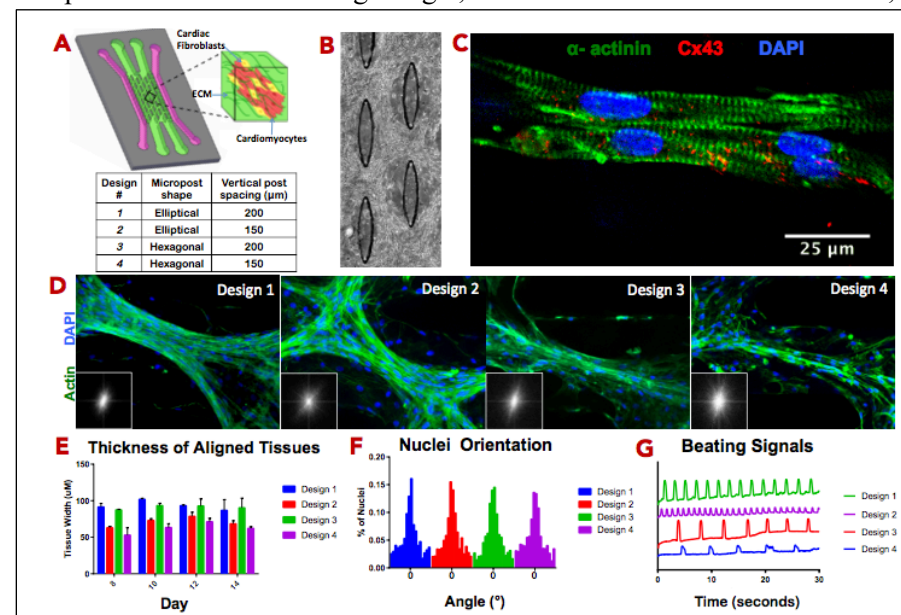


**Figure 1.** A) Schematic of microengineered cardiac platform with table of design dimensions. B) Phase contrast of tissue surrounding microposts within platform. C) Cardiac marker expression within Design 1. D) F-actin (green) and nuclei (blue) of the different designs, with inset of FFT analysis for F-actin. E) Thickness analysis of aligned tissue. F) Orientation of cell nuclei, with  $0^\circ$  as the major alignment axis. G) Representative spontaneous beating signals.

Design 1 were capable of maintaining thicker aligned tissue than the other designs (Fig. 1E), demonstrating its effectiveness in mimicking anisotropy found in native heart tissue architecture. To confirm proper expression of cardiac markers, the tissues were stained for sarcomeric  $\alpha$ -actinin (green) and connexin 43 (red). Fluorescent microscopy revealed striated sarcomeres and abundant expression of cardiac gap junctions (Fig. 1C). These findings demonstrate the feasibility of developing a cardiac tissue model within a microfluidic environment that attains characteristics found in native cardiac tissue.

**Conclusions:** This biomimetic platform proved capable of recapitulating 3D cardiac tissue with optimized structure, cardiac specific markers, and spontaneous contractility over an extended time period. The ongoing work involves the incorporation of hiPSC derived CMs for physiologically relevant human cardiac tissue modeling.

**Acknowledgements:** We would like to acknowledge the NSF CAREER Award #1653193.

The effect of micropost positions was analyzed to assess tissue alignment, cardiac specific markers, and contractility using fluorescence/phase contrast imaging and real time microscopy.

### Results and Discussion:

We microfabricated four designs of optimized micropost positions; all of which demonstrated consistent spontaneous beating (Fig. 1G) over extended culture period (i.e. 14 days). F-actin staining revealed that Design 1 had the highest tissue alignment, further evidenced through Fast Fourier Transform (FFT) analysis (Fig. 1D), as a classical hallmark of native myocardium architecture. Using nuclear orientation analysis to assess alignment, we also found that Design 1 induced the highest percentage of encapsulated cell nuclei in the same orientation along the tissue alignment axis (Fig. 1F).

The specific dimensionalities in